https://doi.org/10.5194/egusphere-2026-3733
Preprint. Discussion started: 27 July 2026

Evaluation of subseasonal sea ice changes in the Community Earth System Model version two

Madeline Frank[1] and Steven M. Cavallo[1]

[1]School of Meteorology, University of Oklahoma, Norman, OK, United States of America

Correspondence: Madeline Frank (madeline.e.frank-1@ou.edu)

Abstract. Forecasting Arctic sea ice is a complex, open problem in polar science, exacerbated by climate change and Arctic amplification. Arctic sea ice dynamics are inherently interconnected to atmosphere and ocean dynamics. This means that coupled climate models are currently the best available tools to model and forecast sea ice. However, climate models consistently underrepresent sea ice processes on subseasonal timescales, contributing to forecasting challenges. In this study, we evaluate the Community Earth System Model Version Two's (CESM2) skill in representing Arctic sea ice by comparing model output to reanalysis and observational data. Doing so establishes CESM2's viability as a tool for studying Arctic sea ice processes and identifies places where model improvements are needed. While sea ice processes in CESM2 have been evaluated on annual and climate timescales, its performance on subseasonal timescales has not. We analyze CESM2's performance in representing subseasonal sea ice variability by comparing its temporal and spatial interannual variability to observations. We also evaluate CESM2's performance at capturing very rapid sea ice loss events (VRILEs). VRILEs are substantial sea ice loss events that occur on the timescale of days. We find that CESM2 does a poor job of representing VRILEs and has less interannual variability than observations.

1 Introduction

The Arctic is a dynamically changing environment, warming at approximately twice the rate as the rest of the world (Solomon et al., 2007; Blunden and Arndt, 2012; Huang et al., 2017). One of the many consequences of accelerated warming in the Arctic is a drastic reduction in both sea ice extent (SIE) and thickness, particularly in the summer (Comiso, 2012; Lindsay and Schweiger, 2015; Kwok, 2018). This sea ice decline has resulted in more open ocean in this region than ever recorded (Stephenson et al., 2013; Stephenson and Smith, 2015), and an increase in the human population (Durkalec et al., 2015). Accurate modeling of Arctic sea ice is necessary for forecasts and projections in this region on both weather and climate scales.

Global climate models have historically been too conservative in their representation of Arctic sea ice's response to climate change (Msadek et al., 2014; Notz and Community, 2020; West and Blockley, 2025). This underestimation is evident in models that fail to capture the observed trends in sea ice, resulting in ice-free summers that are years or even decades later than expected(Notz and Stroeve, 2016; Rosenblum and Eisenman, 2017; Notz and Community, 2020). The Community Earth

https://doi.org/10.5194/egusphere-2026-3733
Preprint. Discussion started: 27 July 2026

System Model Version Two Large Ensemble (CESM2 LENS) (Danabasoglu et al., 2020) is an exception, having an overall negative sea ice bias rooted in insufficient growth of winter ice thickness (DeRepentigny et al., 2020). This negative sea ice bias contrasts with the first version of CESM (CESM-LE), which has a strong positive sea ice bias (DeRepentigny et al., 2020). However, the negative bias in CESM2 can be corrected for by adjusting parameters in the sea ice model physics related to surface albedo, surface melt, sea ice thickness, and summer ice area (Kay et al., 2022) or by using the Whole Atmosphere Community Climate Model version 6 (WACCM6) (Gettelman et al., 2019) instead of the default Community Atmosphere Model version 6 (CAM6) (Danabasoglu et al., 2020) as the model's atmospheric component DeRepentigny et al. (2020).

When WACCM6 is used as CESM2's atmospheric component, the model's representation of sea ice area and volume is comparable to observations (DeRepentigny et al., 2020). The differences in sea ice area and volume between these two model configurations are likely related to the representation of early spring clouds (DeRepentigny et al., 2020). Specifically, CESM2 (CAM6) exhibits thinner clouds in the early spring, which enhances the ice-albedo feedback, ultimately resulting in thinner ice throughout the year (DuVivier et al., 2020). Additionally, they find that CESM2 shows a general improvement over CESM-LE at capturing the September sea ice climate trend and the March sea ice maximum (DeRepentigny et al., 2020). However, the focus of that study was not model performance on subseasonal or shorter timescales, and so it did not address differences at those durations.

Little attention has been given to the model representation of sea ice's interannual variability or performance on subseasonal timescales. In CESM-LE, there are no statistically significant changes in SIE at periods less than 40 days (Cavallo et al., 2025). However, interannual variability is observed to be an important factor in Arctic sea ice trends, both in paleo (Chan et al., 2017; Hörner et al., 2017; Kolling et al., 2018) and satellite era records (Notz and Stroeve, 2018; Roberts et al., 2020). It accounts for 40–50% of the observed multi-decadal trends in Arctic sea ice (Ding et al., 2019) and as much as 60% of the declining trend of September SIE (Ding et al., 2017). March sea ice variability is driven by radiative feedbacks of clouds and water vapor (Luo et al., 2017), surface albedo, surface winds, and oceanic heat transport, while September sea ice interannual variability is primarily driven by surface albedo and fluctuations in temperature advection (Olonscheck et al., 2019). Further complicating matters, the susceptibility of sea ice to internal variability is not spatially uniform (England et al., 2019; Olonscheck et al., 2019). While only 10% of observed sea ice trends in the Eastern Siberian Sea can be attributed to internal variability, that number jumps to over 60% in the Barents and Kara seas (England et al., 2019). The mechanisms behind this interannual variability are not well understood, which represents a significant obstacle for sea ice forecasting.

Some of sea ice's interannual variability can be attributed to teleconnection patterns, specifically the Arctic Oscillation (AO) (Ogi and Wallace, 2007; Knudsen et al., 2015) and the North Atlantic Oscillation (NAO) (Kwok, 2000). Winter and springtime high AO indices tend to be associated with reduced sea ice cover in the eastern Arctic Ocean, Greenland Sea, and Barents Sea (Kwok, 2000). Increased sea ice flux through the Fram Strait is strongly correlated with the positive phase of the NAO (Kwok and Rothrock, 1999). Additionally, persistent anomalies in the upper troposphere, not specifically tied to a known teleconnection pattern, can also affect sea ice. When there is a persistent positive potential temperature anomaly in the upper troposphere in the late spring and early summer, September SIE tends to fall below the climatological trend (Screen et al., 2011). The mechanism behind this relationship is thought to be that the upper-level anomaly leads to fewer clouds and fewer

https://doi.org/10.5194/egusphere-2026-3733
Preprint. Discussion started: 27 July 2026

cyclones over the Arctic, which allows for more direct sunlight on the sea ice, and that this enhanced shortwave radiation leads to enhanced melt from above (Screen et al., 2011). However, late summer cyclones are having an increased effect on sea ice loss in recent decades as ice thickness has waned (Finocchio et al., 2022).

One of the sources of sea ice's short timescale variability are very rapid sea ice loss events (VRILEs) (Cavallo et al., 2025). VRILEs occur on weather timescales and represent statistically significant changes in SIE (Cavallo et al., 2025). Events like these have been observed to be associated with strong Arctic storms driving ocean mixing that increases melt from below (Peng et al., 2021) though there is no consensus on how Arctic cyclones affect sea ice. The effects of a cyclone's dynamics versus thermodynamics can vary with season and tends to affect sea ice asymmetrically, affecting where a VRILE may occur relative to the cyclone center (Clancy et al., 2022). To date, no systematic study has been done on how effectively coupled climate models such as CESM2 represent VRILEs or the processes leading up to them.

In this study, we compare sea ice characteristics in CESM2 LENS with observations from the National Snow and Ice Data Center (NSIDC) (Comiso, 2023) to evaluate CESM2's sea ice performance on subseasonal timescales, with a particular focus on its representation of VRILEs. We also analyze two VRILE case studies, comparing a subseasonal forecast system utilizing CESM2 (Richter et al., 2022) that we refer to as CESM2 S2S in the text. The following section outlines our methodology, Section 3 presents the results, and Section 4 summarizes and contextualizes our findings.

2 Data and Methods

Two sea ice concentration (SIC) datasets are used throughout this study: observations from the National Snow and Ice Data Center (NSIDC) (Comiso, 2023) and an ensemble member from CESM2 LENS (Rodgers et al., 2021). A single member from CESM2 LENS is chosen rather than the ensemble mean because the ensemble mean SIC is outputted monthly, not daily. Daily values are available for individual ensemble members. Because our goal is to quantify CESM2 LENS's general performance in capturing subseasonal sea ice processes, we choose the ensemble member with the highest correlation to the ensemble mean monthly averaged sea ice extent. The ensemble member that meets this criterion is the 17th member started in model year 1301, identifiable by the label “1301.017".

Since the model year in CESM2 LENS does not directly relate to the calendar year, we determine a comparable time period in CESM2 LENS data to NSIDC data from 1980–2020. Figure 1 shows September and March average SIEs in both datasets. These figures illustrate CESM2 LENS's negative bias in SIE that has been well established in previous literature (e.g., Keen et al., 2021; DeRepentigny et al., 2020; DuVivier et al., 2020). CESM2 LENS has its maximum September SIE in 1964 and has a comparable linear climate trend to the NSIDC data in the following decades (Figure 1). Because of CESM2's negative sea ice bias, we prioritized selecting years with the largest sea ice extent because it covers the largest area. Sea ice dynamics are not spatially uniform therefore being able to compare model output to observations in as many locations across the Arctic as possible will give a better overall picture of model performance. Due to these factors, we consider the years 1960-2000 to be the most comparable in CESM2 LENS to the observational period in NSIDC from 1980 to 2020. An additional subset of the CESM2 LENS data is considered from 1910-1950 as representative of model performance without strong climate forcing.

To calculate the power spectrum density (PSD) of the daily change in SIE, the mean is subtracted from the timeseries, and the absolute value of the square of the Fast Fourier Transform is computed. The theoretical red noise spectrum is computed using the lag correlation function for a first-order linear Markov process with a one-lag autocorrelation (Gilman et al., 1963). PSD values greater than the theoretical red noise spectrum are statistically significant at the 95% confidence level.

To evaluate the spatial variability of SIC in CESM2 LENS and NSIDC, we consider the standard deviation at each point in space of the monthly averaged SIC over a 40-year period. The larger the standard deviation at a given point in space, the more interannual variability in SIC at that location. To compare the datasets, we subtract NSIDC from CESM2 LENS. However, since these data are stored on different native grids, we first project the coarse CESM2 LENS data onto NSIDC's grid and then take the difference. Note that for this analysis, the data are not detrended because removing the climate trend would obfuscate the variability being analyzed.

VRILEs are identified in CESM2 LENS data using the same methodology laid out by Cavallo et al. (2025), applying a high-pass filter to remove changes in SIE with a period greater than 18 days. To identify a VRILE's location, we take the five-day change in SIC and identify the largest connected region of loss. The specific location of the VRILE is determined by performing a center of mass calculation within the region of loss, with the percent change in sea ice coverage serving as a proxy for mass.

We utilize CESM2 S2S (Richter et al., 2022) reforecasts to analyze four VRILE cases, comparing the model's performance with that of NSIDC. One summer and one winter VRILEs are selected on both the Atlantic and Pacific sides of the Arctic. Other selection criteria included sea ice loss values close to the mean and occurring within five days of the reforecast initiation. The VRILEs selected, and the associated reforecasts, are detailed in Table 1.

The reforecasts are initialized every Monday from 1999–2020 and run for 45 days. The atmosphere is initialized with NCEP coupled forecast system model version 2 (CFSv2) (Saha et al., 2014), the land with Community Land Model (CLM2) (Lawrence et al., 2019) spun up with CFSv2, and the ocean and sea ice with the Japanese 55-year reanalysis (JRA-55) (Japan Meteorological Agency, Japan, 2013) (Richter et al., 2022). These reforecasts are run with two different atmospheric dynamical cores, CAM6 (Danabasoglu et al., 2020) and WACCM6 (Gettelman et al., 2019). Both datasets are publicly available through CESM. The CAM6 data are available at https://doi.org/10.5065/0s63-m767 and the WACCM6 data are available at https://doi.org/10.5065/ekns-e430.

There are two primary differences between these dynamical cores: vertical depth of the atmosphere and atmospheric chemistry. CAM6 has 32 vertical levels reaching to 3.6 hPa while WACCM6 has 70 vertical levels that extend up to 6 x 10^{-6} hPa. WACCM6 also has interactive chemistry. CESM2 tends to perform better in terms of sea ice with WACCM6 as the atmospheric component rather than CAM6 (DeRepentigny et al., 2020) but the WACCM6 reforecasts do not have full temporal coverage from 1999–2020. A WACCM6 reforecast is not available for the 2007 case.

We select the reforecast initialized closest to the day five days before the VRILE. The December 2011 VRILE came the closest, with model initiation occurring only six days before the VRILE. For the 2007 VRILE, we use the reforecast initialized on 25 June 2007, eight days before the VRILE. Unfortunately, the next reforecast is not initialized until 2 July 2007, which does not provide enough time to evaluate the VRILE that occurred on 3 July. For both the 2012 and 2016 VRILEs, we use

https://doi.org/10.5194/egusphere-2026-3733
Preprint. Discussion started: 27 July 2026

model runs initiated less than five days before the event, only allowing for calculating the three and four-day sea ice changes, respectively. In both instances, using earlier forecasts yielded highly unrealistic results.

Finally, we analyze the difference in sea ice concentration between the reforecast and NSIDC data at the start of the reforecast and on the day of the VRILE. Because these data are on different native grids and have significantly different spatial resolutions, we regrid the CESM2 S2S data onto the finer NSIDC grid before subtracting them.

3 Results

Evaluating the PSDs of the daily change in SIE in CESM2 LENS and NSIDC illustrates the significance of subseasonal sea ice processes in observations and where CESM2 has the greatest room for improvement. At periods greater than 30 days, CESM2 LENS's PSD is nearly identical to NSIDC's (Figure 2). However, their PSDs begin to diverge below 30 days, becoming especially prominent at periods of less than 18 days (Figure 2). It is also of note that NSIDC's PSD has statistically significant peaks at periods less than ten days that are not present in CESM2 LENS (Figure 2). These results are consistent with Figure 2b in Cavallo et al. (2025), which compares the PSD of the daily change in SIE in NSIDC and CESM-LE.

Next, we consider the monthly average SIE. Figures 1 and 3 show several key differences between the CESM2 LENS and observational data. First, there is a strong negative bias in CESM2 LENS SIE in all months (Figure 3). This bias results in ice-free summers, on average, being the norm before present day (DeRepentigny et al., 2020). In NSIDC the September minimum SIE has a linear climate trend with a slope of -0.085×10^6 km^2 per year and an r value of -0.898 for the years 1980-2020 (Figure 1a). The linear trend in CESM2 LENS data for 1960-2000 has a slope of -0.061×10^6 km^2 per year and an r value of -0.841, slightly less than the r value in the NSIDC data (Figure 1a). These findings support similar results regarding CESM2 LENS's representation of sea ice, which generally aligns on annual and climate timescales (e.g. Danabasoglu et al., 2020; Cavallo et al., 2025). In contrast, March SIE shows less similarity between CESM2 LENS and NSIDC. While observations indicate a steady decline in the maximum SIE as well, there is only a slight trend in CESM2 LENS (Figure 1b).

Apart from the overall negative bias, the key difference we observe between the two datasets' daily average SIE is the scale of their inner quartile ranges. For both periods, CESM2 LENS has a much narrower range than NSIDC, with a narrower inner quartile range in the 1910-1950 data (Figure 3a) than the 1960-2000 (Figure 3b), particularly around the March maximum. On average, the difference in SIE between the 75% and 25% bounds in the NSIDC data is 1.245×10^6 km^2 and in CESM2 LENS the difference is 0.698×10^6 km^2. These differences indicate that sea ice in CESM2 LENS exhibits less interannual variability than is observed. This fact, combined with the lack of significant subseasonal changes in SIE in CESM2 LENS (Figure 2) may indicate the importance of such short-term sea ice changes to its overall variability.

The analysis above shows that CESM2 LENS differs from NSIDC in interannual variability and in the representation of sea ice processes with periods of 18 days or less. Now we turn to the analysis of the spatial variability in SIC (Figure 4). We present the data for both CESM2 LENS time periods, but because there is little difference between them, we focus our analysis on the 1960-2000 data.

Figure 4 shows widespread differences in SIC variability between CESM2 LENS and NSIDC. The area between the green and magenta contours in Figure 4 is a proxy for first-year ice and the area poleward of the green contour approximates regions covered by multi-year ice in NSIDC. There are mostly positive values over the regions of multi-year ice. Positive values indicate more interannual variability in SIC in CESM2 LENS than NSIDC. The positive values in the regions of multi-year ice are the result of CESM2 LENS's overall negative bias. These are regions that remain ice-covered year-round in observations but melt in the summer in CESM2 LENS. There are generally negative values over regions of first-year ice, indicating more interannual variability in NSIDC than CESM2 LENS. This indicates that the timing and location of summer sea ice loss vary much more from year to year in observations than in CESM2 LENS. This evidence leads us to conclude CESM2 LENS has less spatial variability in SIC than is observed (Figure 4).

There are a few exceptions to the trend of greater variability in CESM2 LENS compared to NSIDC data in multi-year ice and less variability in first-year ice. In the Eastern Siberia and Laptev Seas in all months (Figure 4) have positive values outside the multi-year ice region indicated by the green contour. In June and August, these appear to be regions of landfast ice, which are known to behave differently from general sea ice trends and can persist throughout the summer in certain locations Eicken et al. (2005). In July, there is a large area in the first-year ice that stretches from the central Arctic, past the 95% SIC contour, to the Siberian coast (Figure 4b and e). This region is associated with the positive values in the multi-year ice and is therefore likely tied to CESM2's overall negative bias as well.

Overall, we find that CESM2 LENS has less spatial variability in SIC than NSIDC throughout the melt season. When these results are considered alongside the PSD of both datasets, two different pictures of how sea ice is lost begin to emerge. For CESM2 LENS, it suggests steady sea ice loss along the sea ice edge. However, the NSIDC data reveal significant contributions to sea ice loss from synoptic-scale processes across various locations throughout the melt season. Since VRILEs are large sea ice losses that occur over short periods of time, they may account for some of the interannual variability in SIC.

Figure 5 shows the number and size of VRILEs per year for a given season. Even though CESM2 LENS does not have significant changes in SIE at short timescales, VRILEs can still be identified using the same criteria as with NSIDC data Cavallo et al. (2025). The key difference between VRILEs in CESM2 LENS and NSIDC is the amount of sea ice loss attributed to each event. VRILEs in CESM2 LENS are approximately an order of magnitude smaller than their observational counterparts (Figure 5). This difference means that nearly one million square kilometers of sea ice loss that occur in short, localized events each year are missing from CESM2 LENS. In the summer, this sea ice loss must be accounted for in other processes, but in the winter, it may not be occurring at all. Winter sea ice loss can lead to an overall increase in sea ice cover as the newly opened areas refreeze Kriegsmann and Brümmer (2014).

3.1 CESM2 Reforecast VRILE Case Studies

This section analyzes the change in SIC and the difference between SIC in the CESM2 S2S reforecast and NSIDC for four VRILE cases: two summer and two winter VRILEs. Figure 6 shows the difference between CESM2 S2S and NSIDC SIC for the day the reforecast was initialized and the day the VRILE occurs and the five day change (or difference between the day the

https://doi.org/10.5194/egusphere-2026-3733
Preprint. Discussion started: 27 July 2026

VRILE occurs and the day the reforecast is initialized when less than five days of data is available before the VRILE) for all four cases.

3.1.1 3 July 2007 VRILE

The VRILE on 3 July 2007 occurs in the Kara Sea. In the initial difference between the reforecast and NSIDC, there are broad differences along the sea ice edge (Figure 6a). While CESM2 initially has too much sea ice at the VRILE location, there are also locations where it has too little sea ice relative to NSIDC. However, by the time the VRILE occurs, the reforecast only has positive differences, especially in the region of the VRILE (Figure 6g). This means that not only is the VRILE too small, but there is too little ice loss Arctic-wide during this time period. Given CESM2 LENS's overall negative sea ice bias, one might anticipate aggressive seasonal losses; however, that is not the case here.

The five-day change in SIC in the reforecast shows a region of loss in the correct location that, in the SIE data, accounts for approximately 0.12×10^6 square kilometers of sea ice loss. In observations, this VRILE accounts for $\approx 0.29 \times 10^6$ square kilometers of sea ice loss, but there are other VRILEs associated with ice loss around 0.12×10^6. Thus, while the estimated sea ice loss by CESM2 in this case is too low, it is within the typical range of VRILEs. This is not the case for any VRILE identified in CESM2 LENS (Figure 5).

3.1.2 11 December 2011 VRILE

The 11 December 2011 case is a wintertime VRILE in the Bering Sea. Over the five-day period, there is near ubiquitous sea ice growth in both atmospheric configurations (Figure 6n,o), which is appropriate for this time of year, given that air temperatures are well below freezing. In the CAM6 run, there is no region of sea ice loss (Figure 6n), but the WACCM6 reforecast indicates a small region of sea ice loss co-located with the VRILE in NSIDC data (Figure 6o). Both reforecasts have too little sea ice along Alaska's western coast at the start of the reforecast (Figure 6b,c). On the day of the VRILE, the WACCM6 run still has too little sea ice in that region (Figure 6i), but the CAM6 run has too much relative to NSIDC (Figure 6h).

The CAM6 scenario can be interpreted as the change in sea ice concentration in the VRILE region (Figure 6b) as beginning with too little sea ice and experiencing sea ice growth consistent with the seasonal trend. Since there is a positive SIC anomaly in the reforecast relative to observations at the time of the VRILE (Figure 6h), we can infer that the model's seasonal trend is dominating the shorter timescale process that would otherwise result in a temporary loss in that region.

However, in the WACCM6 scenario, there is loss in that region (Figure 6i). Here, the short-term process is visible, unlike in the CAM6 run. The scenario both begins and ends with too little sea ice at the VRILE location relative to NSIDC, but there is still some loss despite the seasonal trend. Since the WACCM6 scenario has a smaller negative difference in sea ice concentration from NSIDC on the day of the VRILE than in its initial conditions, its VRILE still did not lose enough sea ice. If it had, the initial difference in sea ice between the WACCM6 scenario and NSIDC would have been approximately the same as the difference between them at the time of the VRILE.

https://doi.org/10.5194/egusphere-2026-3733
Preprint. Discussion started: 27 July 2026

3.2 9 August 2012 VRILE

The 9 August 2012 VRILE is associated with the Great Arctic Cyclone of 2012 (GAC2012) (Simmonds and Rudeva, 2012). The reforecast closest to the VRILE was initialized on 6 August 2012, which only allows for a three-day change in SIC. However, the previous reforecast, initialized on 30 July 2012, GAC2012 was not present at all. In fact there was a weak high pressure system present where GAC2012 should have been. Consequently, we present results from the 6 August 2012 reforecast. This reforecast did capture GAC2012 though it was weaker than in ERA5 reanalysis. Though the 30 July results are not shown, there were no major qualitative differences between either run's representation of the VRILE.

At initiation, CESM2 S2S has too little sea ice over most of the Arctic relative to NSIDC, especially on the Pacific side (Figure 6 d). This negative bias persists relatively unchanged throughout the day of the VRILE (Figure 6 j). This is likely due in part to the seasonal melting trend. CESM2 loses sea ice over this period in the central Arctic, but has a small amount of sea ice gain at the VRILE location (Figure 6p). This pattern is not representative of the sea ice loss associated with GAC2012.

3.2.1 23 December 2016 VRILE

The 23 December 2016 VRILE is in the Kara Sea. The primary differences in SIC between the model output and NSIDC for both the CAM6 and WACCM6 reforecasts are at the location of the VRILE and in Hudson Bay, with too much sea ice relative to observations at the VRILE location and too little in Hudson Bay (Figure 6 e, f, k, and l). For both atmospheric configurations, there is sea ice loss at the VRILE location over the five-day period, though the negative change is larger in the CAM6 run than in WACCM6 (Figure 6 q and r). Additionally, both runs show a larger positive SIC anomaly at the VRILE location at the time of the VRILE than at initialization (Figure 6 k and l). These patterns suggest that neither reforecasts lost enough sea ice over this time period. If they had lost a similar amount of sea ice as the VRILE in observations, we would expect to see similar differences between the reforecasts and NSIDC at the initial conditions and at the time of the VRILE.

While the CAM6 run captures sea ice loss at the VRILE location and exhibits a more negative change than the WACCM6 run, it also shows unseasonal ice loss along the entire sea ice edge (Figure 6 q and r). The WACCM6 reforecast seems to correct its negative sea ice anomaly relative to NSIDC in Hudson Bay and, with the exception of the VRILE location, has Arctic-wide sea ice gain. Therefore, while the WACCM6 reforecast does a better job of capturing sea ice behavior Arctic-wide, its VRILE is still much too small (Figure 6r).

There are several commonalities between these four VRILE cases. Generally, the reforecasts often capture some sea ice loss in the correct region, but it is much too small of a change to reflect the observed magnitudes of VRILEs. It is worth noting that there is a lack of coupled ocean wave-sea ice dynamics in the reforecast model. This issue may also be related to model resolution. CESM2's has grid spacing is approximately 50 km (Kay et al., 2015), but sea ice floes and the ocean waves are on the order of 100 m. Additionally, low-level jets that can drive these ocean sea ice dynamics require $\Delta x \approx 17-23$ km to resolve, with peak winds occurring on even smaller scales (Guest et al., 2018). For global climate models, these resolution issues highlight the need to reassess how the affected processes are handled in the model's parameterization schemes.

https://doi.org/10.5194/egusphere-2026-3733
Preprint. Discussion started: 27 July 2026

4 Conclusions

The purpose of this paper is to evaluate CESM2's skill in representing subseasonal sea ice processes. CESM2 is one of the few models that joins sea ice to the atmosphere and ocean, a necessary element given sea ice's highly coupled nature. Most of the previous work in this area has focused on model performance at climate timescales. Our aim in evaluating sea ice in CESM2 at subseasonal timescales is twofold: to determine if CESM2 is an effective tool for studying short timescale sea ice processes such as VRILEs and to identify processes that may affect how sea ice is represented on interannual and climate scales. Our primary findings are that CESM2 largely does not capture VRILEs or synoptic-scale sea ice changes generally and that the model has less interannual variability both spatially and temporally than observations.

Overall, these results present a picture of sea ice being lost and gained steadily at the edges in CESM2 LENS, behaving much like a single, large block of ice. There may be small variations from day to day and region to region, but these have a minimal effect on the overall behavior of the sea ice. This picture contrasts with SIC in NSIDC, where daily and regional differences can be significant. The significance of these local, short timescale processes aligns with previous observational studies (e.g. Asplin et al., 2012, 2014; Collins III et al., 2015) and is supported by the prevalence of VRILEs Cavallo et al. (2025). Together, these points suggest that the key to future improvements in sea ice modeling may lie in how synoptic-scale processes are represented. This is certainly necessary to skillfully forecast sea ice for the shipping industry and other stakeholders.

Moving forward, it is crucial to identify which processes are currently missing from sea ice models. But before that can happen, more work is needed to understand the physical drivers behind synoptic-scale sea ice loss. While at seasonal timescales and longer, sea ice loss is primarily driven by atmospheric heating, losses at shorter timescales may also depend on oceanic heat transport through vertical mixing and ocean wave dynamics. Categorizing the relative importance of these processes and identifying any other important factors at these shorter timescales is necessary before model improvements can be made.

Data availability. This study uses data from CESM2 LENS, CESM2 S2S, and NSIDC. CESM2 LENS data is available through the National Center for Atmospheric Research's (NCAR) Climate Data Gateway at https://www.cesm.ucar.edu/projects/community-projects/LENS2/data-sets.html. The CESM2 S2S reforecasts are available through the Climate Data Gateway https://doi.org/10.5065/0s63-m767. NSIDC sea ice concentration data is available through NASA National Snow and Ice Data Center Distributed Active Archive Center https://doi.org/10.5067/X5LG68MH013O.

Author contributions. All co-authors were involved in the conceit of the analysis. MF performed the data analysis, and SC provided contributions. MF prepared the manuscript with SC providing significant revisions.

Competing interests. There are no competing interests present.

https://doi.org/10.5194/egusphere-2026-3733
Preprint. Discussion started: 27 July 2026

Acknowledgements. We thank the Office of Naval Research for support of this research under ONR grant N00014-18-1-2223.

References

Asplin, M. G., Galley, R., Barber, D. G., and Prinsenberg, S.: Fracture of summer perennial sea ice by ocean swell as a result of Arctic storms, Journal of Geophysical Research: Oceans, 117, 2012.

Asplin, M. G., Scharien, R., Else, B., Howell, S., Barber, D. G., Papakyriakou, T., and Prinsenberg, S.: Implications of fractured Arctic perennial ice cover on thermodynamic and dynamic sea ice processes, Journal of Geophysical Research: Oceans, 119, 2327–2343, 2014.

Blunden, J. and Arndt, D. S.: State of the climate in 2011, Bulletin of the American Meteorological Society, 93, S1–S282, 2012.

Cavallo, S. M., Frank, M. C., and Bitz, C. M.: Sea ice loss in association with Arctic cyclones, Communications Earth & Environment, 6, 44, 2025.

Chan, P., Halfar, J., Adey, W., Hetzinger, S., Zack, T., Moore, G., Wortmann, U., Williams, B., and Hou, A.: Multicentennial record of Labrador Sea primary productivity and sea-ice variability archived in coralline algal barium, Nature communications, 8, 1–10, 2017.

Clancy, R., Bitz, C. M., Blanchard-Wrigglesworth, E., McGraw, M. C., and Cavallo, S. M.: A cyclone-centered perspective on the drivers of asymmetric patterns in the atmosphere and sea ice during Arctic cyclones, Journal of Climate, 35, 73–89, 2022.

Collins III, C. O., Rogers, W. E., Marchenko, A., and Babanin, A. V.: In situ measurements of an energetic wave event in the Arctic marginal ice zone, Geophysical Research Letters, 42, 1863–1870, 2015.

Comiso, J.: Bootstrap Sea Ice Concentrations from Nimbus-7 SMMR and DMSP SSM/I-SSMIS, Version 4, https://doi.org/10.5067/X5LG68MH013O, 2023.

Comiso, J. C.: Large decadal decline of the Arctic multiyear ice cover, Journal of Climate, 25, 1176–1193, 2012.

Danabasoglu, G., Lamarque, J.-F., Bacmeister, J., Bailey, D., DuVivier, A., Edwards, J., Emmons, L., Fasullo, J., Garcia, R., Gettelman, A., et al.: The community earth system model version 2 (CESM2), Journal of Advances in Modeling Earth Systems, 12, e2019MS001 916, 2020.

DeRepentigny, P., Jahn, A., Holland, M. M., and Smith, A.: Arctic sea ice in two configurations of the CESM2 during the 20th and 21st centuries, Journal of Geophysical Research: Oceans, 125, e2020JC016 133, 2020.

Ding, Q., Schweiger, A., L'Heureux, M., Battisti, D. S., Po-Chedley, S., Johnson, N. C., Blanchard-Wrigglesworth, E., Harnos, K., Zhang, Q., Eastman, R., et al.: Influence of high-latitude atmospheric circulation changes on summertime Arctic sea ice, Nature Climate Change, 7, 289–295, 2017.

Ding, Q., Schweiger, A., L'Heureux, M., Steig, E. J., Battisti, D. S., Johnson, N. C., Blanchard-Wrigglesworth, E., Po-Chedley, S., Zhang, Q., Harnos, K., et al.: Fingerprints of internal drivers of Arctic sea ice loss in observations and model simulations, Nature Geoscience, 12, 28–33, 2019.

Durkalec, A., Furgal, C., Skinner, M. W., and Sheldon, T.: Climate change influences on environment as a determinant of Indigenous health: Relationships to place, sea ice, and health in an Inuit community, Social science & medicine, 136, 17–26, 2015.

DuVivier, A. K., Holland, M. M., Kay, J. E., Tilmes, S., Gettelman, A., and Bailey, D. A.: Arctic and Antarctic sea ice mean state in the Community Earth System Model version 2 and the influence of atmospheric chemistry, Journal of Geophysical Research: Oceans, 125, e2019JC015 934, 2020.

Eicken, H., Dmitrenko, I., Tyshko, K., Darovskikh, A., Dierking, W., Blahak, U., Groves, J., and Kassens, H.: Zonation of the Laptev Sea landfast ice cover and its importance in a frozen estuary, Global and planetary change, 48, 55–83, 2005.

England, M., Jahn, A., and Polvani, L.: Nonuniform contribution of internal variability to recent Arctic sea ice loss, Journal of Climate, 32, 4039–4053, 2019.

https://doi.org/10.5194/egusphere-2026-3733
Preprint. Discussion started: 27 July 2026

Finocchio, P. M., Doyle, J. D., and Stern, D. P.: Accelerated sea ice loss from late summer cyclones in the new Arctic, Journal of Climate, 35, 7751–7769, 2022.

Gettelman, A., Mills, M., Kinnison, D., Garcia, R., Smith, A., Marsh, D., Tilmes, S., Vitt, F., Bardeen, C., McInerny, J., et al.: The whole atmosphere community climate model version 6 (WACCM6), Journal of Geophysical Research: Atmospheres, 124, 12 380–12 403, 2019.

Gilman, D. L., Fuglister, F. J., and Mitchell, J.: On the power spectrum of "red noise", Journal of the Atmospheric Sciences, 20, 182–184, 1963.

Guest, P., Persson, P. O. G., Wang, S., Jordan, M., Jin, Y., Blomquist, B., and Fairall, C.: Low-level baroclinic jets over the new Arctic Ocean, Journal of Geophysical Research: Oceans, 123, 4074–4091, 2018.

Hörner, T., Stein, R., and Fahl, K.: Evidence for Holocene centennial variability in sea ice cover based on IP25 biomarker reconstruction in the southern Kara Sea (Arctic Ocean), Geo-Marine Letters, 37, 515–526, 2017.

Huang, J., Zhang, X., Zhang, Q., Lin, Y., Hao, M., Luo, Y., Zhao, Z., Yao, Y., Chen, X., Wang, L., et al.: Recently amplified arctic warming has contributed to a continual global warming trend, Nature climate change, 7, 875–879, 2017.

Japan Meteorological Agency, Japan: JRA-55: Japanese 55-year Reanalysis, Monthly Means and Variances, https://doi.org/10.5065/D60G3H5B, 2013.

Kay, J. E., Deser, C., Phillips, A., Mai, A., Hannay, C., Strand, G., Arblaster, J. M., Bates, S., Danabasoglu, G., Edwards, J., et al.: The Community Earth System Model (CESM) large ensemble project: A community resource for studying climate change in the presence of internal climate variability, Bulletin of the American Meteorological Society, 96, 1333–1349, 2015.

Kay, J. E., DeRepentigny, P., Holland, M. M., Bailey, D. A., DuVivier, A. K., Blanchard-Wrigglesworth, E., Deser, C., Jahn, A., Singh, H., Smith, M. M., et al.: Less surface sea ice melt in the CESM2 improves Arctic sea ice simulation with minimal non-polar climate impacts, Journal of Advances in Modeling Earth Systems, 14, e2021MS002 679, 2022.

Keen, A., Blockley, E., Bailey, D. A., Boldingh Debernard, J., Bushuk, M., Delhaye, S., Docquier, D., Feltham, D., Massonnet, F., O'Farrell, S., et al.: An inter-comparison of the mass budget of the Arctic sea ice in CMIP6 models, The Cryosphere, 15, 951–982, 2021.

Knudsen, E. M., Orsolini, Y. J., Furevik, T., and Hodges, K. I.: Observed anomalous atmospheric patterns in summers of unusual Arctic sea ice melt, Journal of Geophysical Research: Atmospheres, 120, 2595–2611, 2015.

Kolling, H. M., Stein, R., Fahl, K., Perner, K., and Moros, M.: New insights into sea ice changes over the past 2.2 kyr in Disko Bugt, West Greenland, arktos, 4, 1–20, 2018.

Kriegsmann, A. and Brümmer, B.: Cyclone impact on sea ice in the central Arctic Ocean: a statistical study, The Cryosphere, 8, 303, 2014.

Kwok, R.: Recent changes in Arctic Ocean sea ice motion associated with the North Atlantic Oscillation, Geophysical Research Letters, 27, 775–778, 2000.

Kwok, R.: Arctic sea ice thickness, volume, and multiyear ice coverage: losses and coupled variability (1958–2018), Environmental Research Letters, 13, 105 005, 2018.

Kwok, R. and Rothrock, D. A.: Variability of Fram Strait ice flux and North Atlantic oscillation, Journal of Geophysical Research: Oceans, 104, 5177–5189, 1999.

Lawrence, D. M., Fisher, R. A., Koven, C. D., Oleson, K. W., Swenson, S. C., Bonan, G., Collier, N., Ghimire, B., van Kampenhout, L., Kennedy, D., et al.: The Community Land Model version 5: Description of new features, benchmarking, and impact of forcing uncertainty, Journal of Advances in Modeling Earth Systems, 11, 4245–4287, 2019.

Lindsay, R. and Schweiger, A.: Arctic sea ice thickness loss determined using subsurface, aircraft, and satellite observations, The Cryosphere, 9, 269–283, 2015.

Luo, B., Luo, D., Wu, L., Zhong, L., and Simmonds, I.: Atmospheric circulation patterns which promote winter Arctic sea ice decline, Environmental Research Letters, 12, 054 017, 2017.

Msadek, R., Vecchi, G., Winton, M., and Gudgel, R.: Importance of initial conditions in seasonal predictions of Arctic sea ice extent, Geophysical Research Letters, 41, 5208–5215, 2014.

Notz, D. and Community, S.: Arctic sea ice in CMIP6, Geophysical Research Letters, 47, e2019GL086 749, 2020.

Notz, D. and Stroeve, J.: Observed Arctic sea-ice loss directly follows anthropogenic CO2 emission, Science, 354, 747–750, 2016.

Notz, D. and Stroeve, J.: The trajectory towards a seasonally ice-free Arctic Ocean, Current Climate Change Reports, 4, 407–416, 2018.

Ogi, M. and Wallace, J. M.: Summer minimum Arctic sea ice extent and the associated summer atmospheric circulation, Geophysical Research Letters, 34, 2007.

Olonscheck, D., Mauritsen, T., and Notz, D.: Arctic sea-ice variability is primarily driven by atmospheric temperature fluctuations, Nature Geoscience, 12, 430–434, 2019.

Peng, L., Zhang, X., Kim, J.-H., Cho, K.-H., Kim, B.-M., Wang, Z., and Tang, H.: Role of intense Arctic storm in accelerating summer sea ice melt: An in situ observational study, Geophysical Research Letters, 48, e2021GL092 714, 2021.

Richter, J. H., Glanville, A. A., Edwards, J., Kauffman, B., Davis, N. A., Jaye, A., Kim, H., Pedatella, N. M., Sun, L., Berner, J., et al.: Subseasonal Earth system prediction with CESM2, Weather and Forecasting, 37, 797–815, 2022.

Roberts, M. J., Jackson, L. C., Roberts, C. D., Meccia, V., Docquier, D., Koenigk, T., Ortega, P., Moreno-Chamarro, E., Bellucci, A., Coward, A., et al.: Sensitivity of the Atlantic meridional overturning circulation to model resolution in CMIP6 HighResMIP simulations and implications for future changes, Journal of Advances in Modeling Earth Systems, 12, e2019MS002 014, 2020.

Rodgers, K. B., Lee, S.-S., Rosenbloom, N., Timmermann, A., Danabasoglu, G., Deser, C., Edwards, J., Kim, J.-E., Simpson, I. R., Stein, K., et al.: Ubiquity of human-induced changes in climate variability, Earth System Dynamics, 12, 1393–1411, 2021.

Rosenblum, E. and Eisenman, I.: Sea ice trends in climate models only accurate in runs with biased global warming, Journal of Climate, 30, 6265–6278, 2017.

Saha, S., Moorthi, S., Wu, X., Wang, J., Nadiga, S., Tripp, P., Behringer, D., Hou, Y.-T., Chuang, H.-y., Iredell, M., et al.: The NCEP climate forecast system version 2, Journal of climate, 27, 2185–2208, 2014.

Screen, J. A., Simmonds, I., and Keay, K.: Dramatic interannual changes of perennial Arctic sea ice linked to abnormal summer storm activity, Journal of Geophysical Research: Atmospheres, 116, 2011.

Simmonds, I. and Rudeva, I.: The great Arctic cyclone of August 2012, Geophysical research letters, 39, 2012.

Solomon, S., Qin, D., Manning, M., Averyt, K., and Marquis, M.: Climate change 2007-the physical science basis: Working group I contribution to the fourth assessment report of the IPCC, vol. 4, Cambridge university press, 2007.

Stephenson, S. R. and Smith, L. C.: Influence of climate model variability on projected Arctic shipping futures, Earth's Future, 3, 331–343, 2015.

Stephenson, S. R., Smith, L. C., Brigham, L. W., and Agnew, J. A.: Projected 21st-century changes to Arctic marine access, Climatic Change, 118, 885–899, 2013.

West, A. E. and Blockley, E. W.: CMIP6 models overestimate sea ice melt, growth and conduction relative to ice mass balance buoy estimates, Geoscientific Model Development, 18, 3041–3064, 2025.

https://doi.org/10.5194/egusphere-2026-3733
Preprint. Discussion started: 27 July 2026

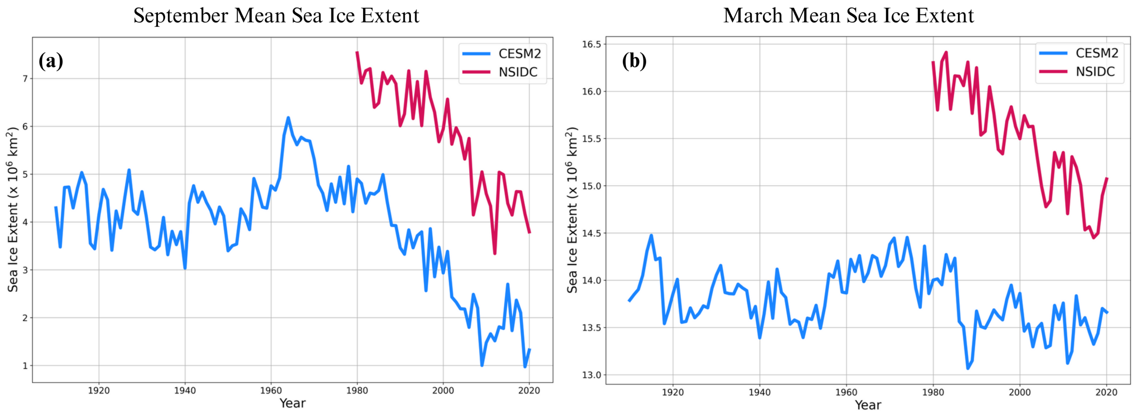

Figure 1. September (a) and March (b) average sea ice extent for CESM2 LENS (pink) and NSIDC (blue). CESM2 LENS data is from 1900-2020 and NSIDC data from 1980-2020.

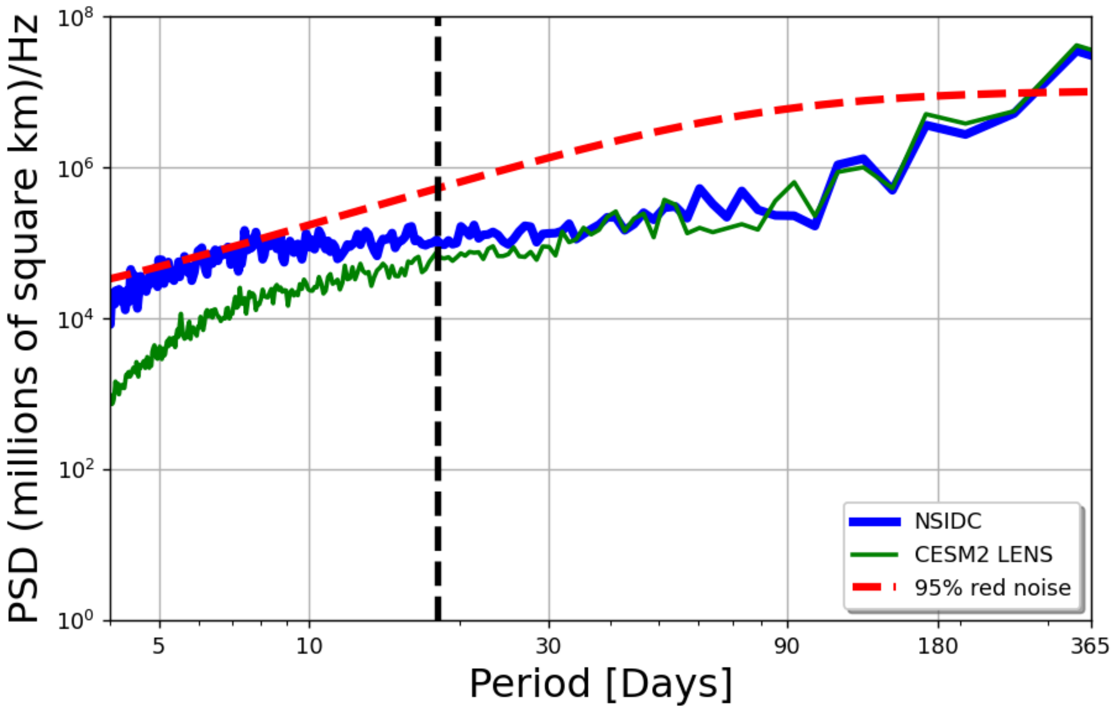

Figure 2. Daily change in sea ice extent power spectral density (PSD) for CESM2 (green) large ensemble member closest to its ensemble mean compared to observations from the NSIDC sea ice index (blue). The 95% confidence interval from the theoretical red noise spectrum (dashed red) is also shown. The vertical dashed black line denotes the 18-day cutoff period used to identify VRILEs.

https://doi.org/10.5194/egusphere-2026-3733
Preprint. Discussion started: 27 July 2026

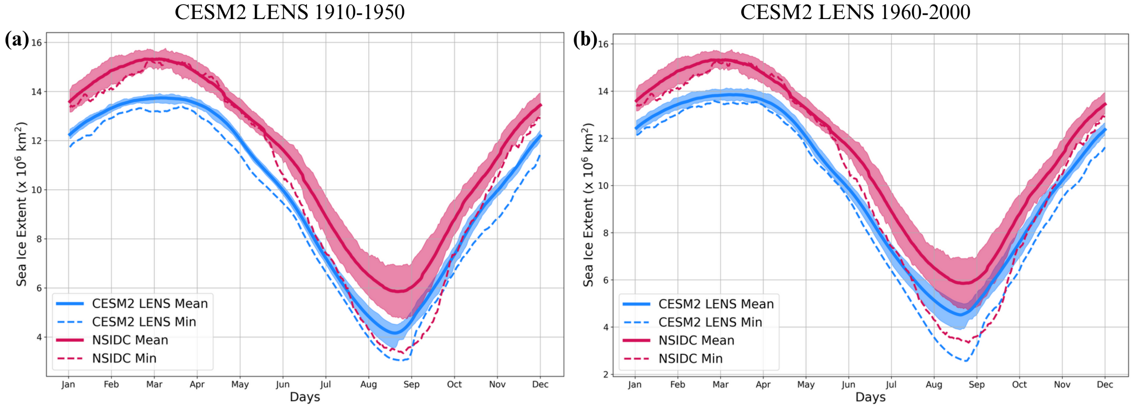

Figure 3. Daily average sea ice extent for CESM2 LENS (pink) and NSIDC (blue). Mean values are plotted with a solid line. The year with the minimum September extent is plotted as the dotted lines. Shading indicates the inner quartile range. The NSIDC data in (a) and (b) are from 1980-2020 while (a) uses CESM2 LENS data from 1910-1950 and (b) from 1960-2000.

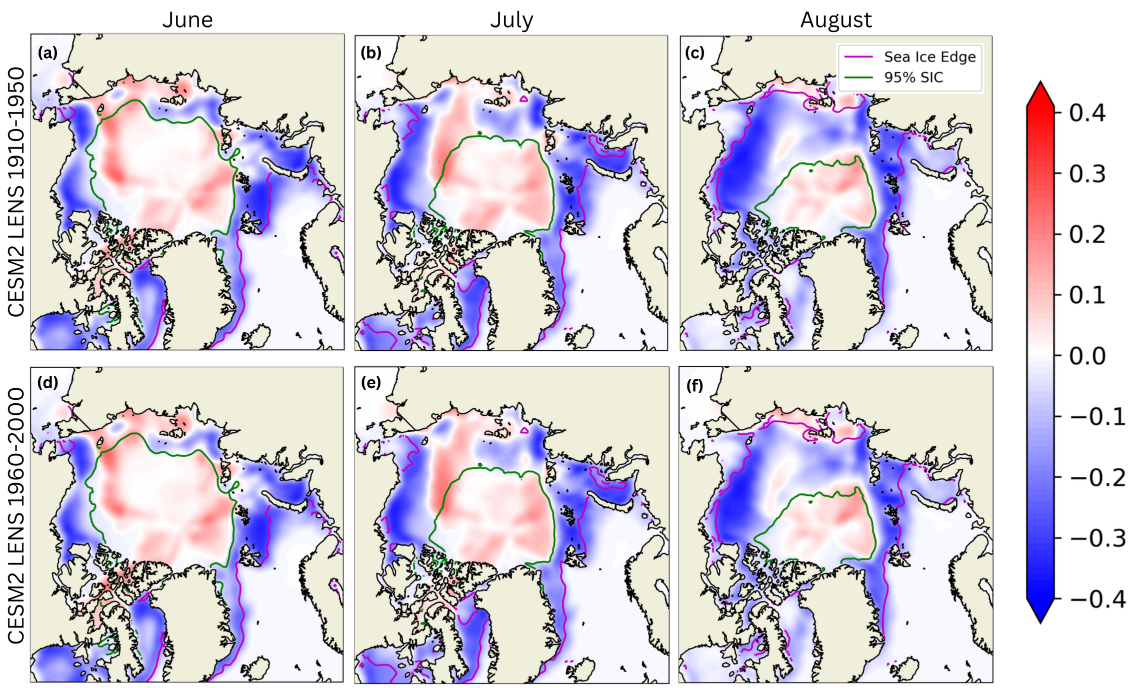

Figure 4. Difference between CESM2 LENS and NSIDC's standard deviation of monthly average SIC. The differences for June (a and d), July (b and e), and August (c and f) are shown for CESM2 LENS years 1910-1950 (a-c) and 1960-2000 (d-f). Positive (negative) values indicate that CESM2 LENS data has a larger (smaller) standard deviation than NSIDC. The NSIDC climatological monthly mean (1990-2020) sea ice edge, taken to be the 0.15 SIC contour, is shown in pink, and the climatological mean 0.95 SIC contour in green.

https://doi.org/10.5194/egusphere-2026-3733
Preprint. Discussion started: 27 July 2026

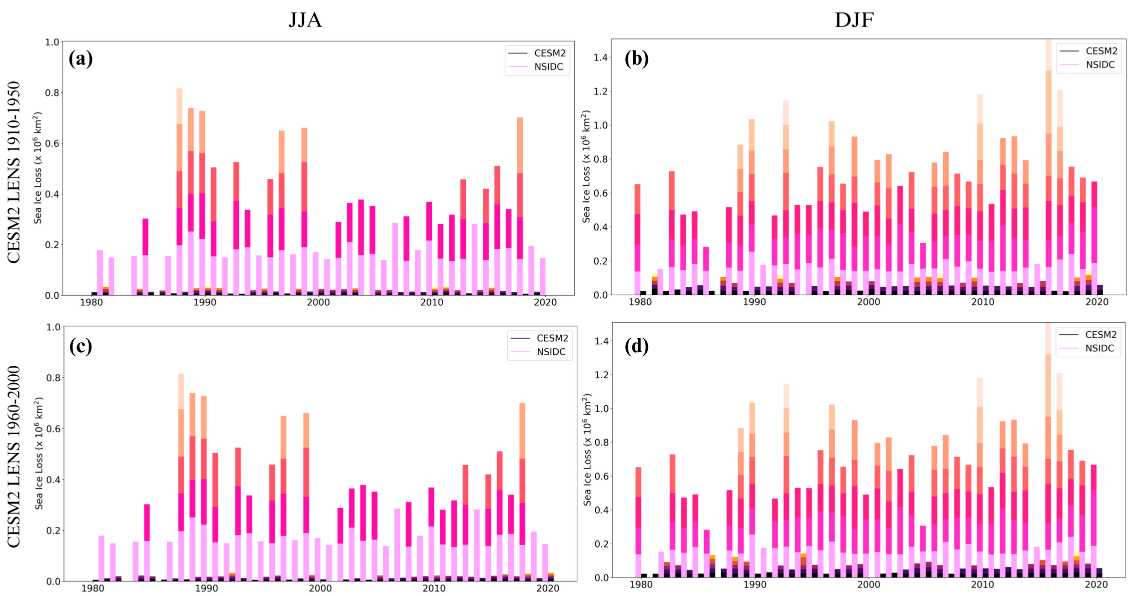

Figure 5. VRILE size by year in NSIDC (pinks) and CESM2 (blues) for summer (jja) in (a) and (c) and winter (djf) in (b) and (d). In years with multiple VRILEs, the sea ice losses are vertically stacked, each color representing a unique VRILE. Figures (a) and (b) use CESM2 data from 1910-1950 while (c) and (d) use 1960-2000.

VRILE Cases			
Season	Region	VRILE Date	Model Initialization
Summer	Atlantic	3 July 2007	25 June 2007
Summer	Pacific	9 August 2012	6 August 2012
Winter	Atlantic	23 December 2016	19 December 2016
Winter	Pacific	11 December 2011	5 December 2011

Table 1. Date and region of VRILE cases and initialization date for CESM2 S2S reforecasts.

https://doi.org/10.5194/egusphere-2026-3733
Preprint. Discussion started: 27 July 2026

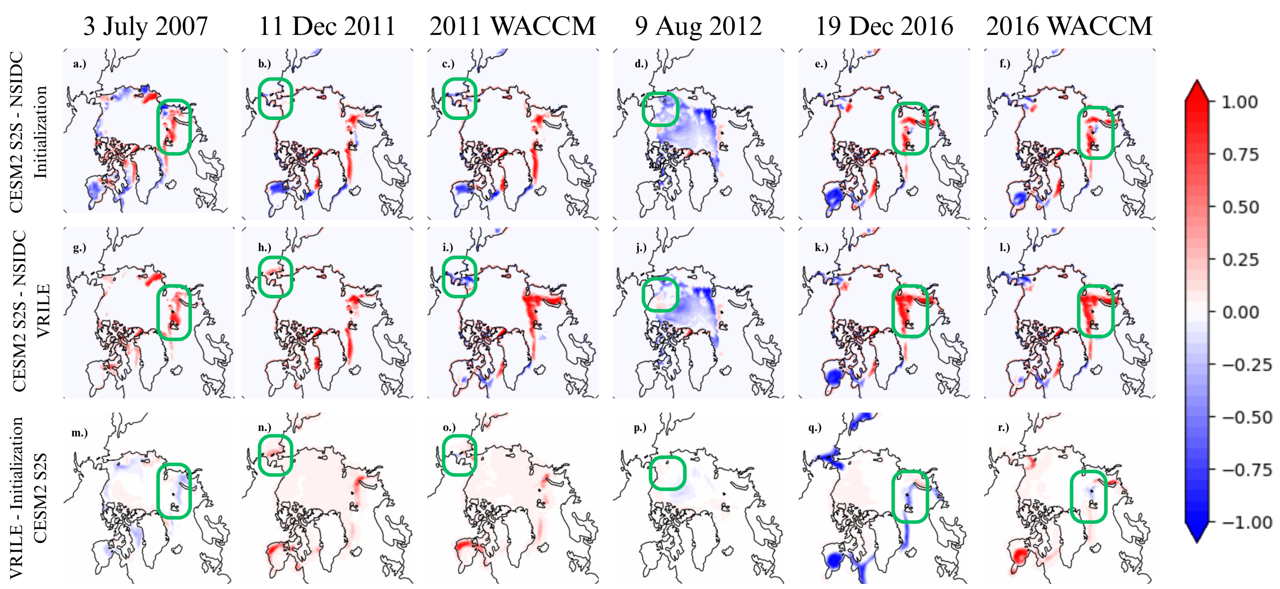

Figure 6. Difference between SIC in CESM2 S2S reforecasts and NSIDC on the day the reforecast was initialized (first row), the day the subsequent VRILE occurred (second row) and the five day change in SIC in CESM2 S2S (third row). These differences are for four different VRILEs that occurred on the date indicated by the column header. For the 11 Dec 2011 and 19 Dec 2016 VRILEs, data was available for both the CAM6 and WACCM6 atmospheric configurations and so the differences for both configurations are shown. The location of the VRILE is circled in green on each plot.